

# Persistence-based Line Detection in Hough Space

Johannes Ferner<sup>1\*</sup>, Stefan Huber<sup>1,2\*</sup>, Saverio Messineo<sup>1,2\*</sup>, Angel Pop<sup>1,2\*</sup>, and  
Martin Uray<sup>1,2\*</sup>

<sup>1</sup> Department for Information Technologies and Digitalisation,

<sup>2</sup> Josef Ressel Centre for Intelligent and Secure Industrial Automation,  
Salzburg University of Applied Sciences, Puch bei Hallein, Austria  
{j.ferner.itsb-m2023, stefan.huber, saverio.messineo, angel-ioan.pop,  
martin.uray}@fh-salzburg.ac.at

**Abstract.** The Hough transform is a popular and classical technique in computer vision for the detection of lines (or more general objects). It maps a pixel into a dual space – the Hough space: each pixel is mapped to the set of lines through this pixel, which forms a curve in Hough space. The detection of lines then becomes a *voting* process to find those lines that received many votes by pixels. However, this voting is done by thresholding, which is susceptible to noise and other artifacts.

In this work, we present an alternative voting technique to detect peaks in the Hough space based on persistent homology, which very naturally addresses limitations of simple thresholding. Experiments on synthetic data show that our method significantly outperforms the original method, while also demonstrating enhanced robustness.

This work seeks to inspire future research in two key directions. First, we highlight the untapped potential of Topological Data Analysis techniques and advocate for their broader integration into existing methods, including well-established ones.

Secondly, we initiate a discussion on the mathematical stability of the Hough transform, encouraging exploration of mathematically grounded improvements to enhance its robustness.

**Keywords:** Hough Transform · Line Detection · Persistent Homology · Topological Data Analysis.

## 1 Introduction

Line detection is a fundamental task in computer vision and pattern recognition, and the *Hough transform* is a classical and most widely used technique for it [11]. It maps sampled points from the image space into a dual representation known as the Hough space or parameter space, which is the space of lines, where each point is mapped to the set of all possible lines passing through it. The line detection is then performed by applying a threshold to vote counts in this space [5], i.e., to

---

\* Authors listed in alphabetical order. J. Ferner and A. Pop contributed equally to this work. M. Uray is the corresponding author. Manuscript accepted at the 6<sup>th</sup> Interdisciplinary Data Science Conference (iDSC’25).

find the lines that were voted most by points. Existing state-of-the-art methods typically either rely on problem-dependent thresholds that require tuning or on computationally expensive approaches, such as machine learning, to identify *relevant* lines.

A key limitation of the Hough transform is its sensitivity to threshold selection, with no universal value due to factors like noise, parallel line proximity, and straightness deviation. Various heuristics and multi-parameter methods have been proposed to address this issue, but they inevitably introduce further parameters that require tuning, making them equally sensitive to varying conditions.

In this paper we revisit the core problem: identifying lines within the Hough space by finding the “relevant” peaks in the accumulation of votes in the Hough space. This accumulation can be seen as a landscape, a scalar field, in which we aim to identify the most “prominent” peaks.

However, the most prominent peaks are not necessarily the highest ones, as found by thresholding. This is analogous to alpinism, where a large rock close to a mountain peak may not be considered a mountain on its own. To make this notion of “prominence” precise we use the mathematical framework of Persistent Homology (PH), which has already been used in other domains for robust peak detection, cf. [9].

This work makes the following key contributions:

- a.) We introduce a novel approach that integrates PH into the widely used Hough transform, improving robustness against noise and reducing needs for parameter tuning.
- b.) Within our experimental scenarios, our method empirically outperforms the original line detection method with respect to stability against noise and robustness against different number of samples for different lines.
- c.) We experimentally provide evidence for *Lipschitz stability* for the proposed method.

In Section 2 we give an overview of the line detection using the Hough transform and PH, before describing related adaptations to the Hough transform in Hough space in Section 3. We continue by introducing our proposed method in Section 4, before evaluating the proposed approach in Section 5. The results, limitations and further potential are discussed in Section 6.

## 2 Preliminaries

This section will introduce the theoretical background for line detection using the Hough transform (Section 2.1) and PH (Section 2.2). In the following description, we limit the formal details to a level necessary for the remaining work. For further details, the reader is referred to the cited literature.

### 2.1 Line Detection using the Hough Transform

For the line detection using the Hough transform [5], we consider a binarized input image  $P = \{(x_i, y_i) \mid 1 \leq i \leq M\}$ , where  $M$  is the number of points in the

image, in which lines are to be detected. A straight line can be parametrized by two parameters in different ways. We use the orthogonal supporting vector in polar coordinates  $(\rho, \theta)$ . The Hough space  $S$  is then the  $\rho$ - $\theta$ -plane; each point in it describes a line in the image space. Note that each image point  $(x, y)$  on a line parametrized by  $(\rho, \theta)$  fulfills  $\rho = x \cos \theta + y \sin \theta$ . In other words, the set of lines through an image point  $(x_i, y_i)$  forms in a sinusoidal curve  $\rho = x_i \cos \theta + y_i \sin \theta$  in the Hough space, cf. Figure 1.

If the image points lie on a straight line  $(\rho, \theta)$  in image space  $I$  then their corresponding curves in Hough space intersect at a common point  $(\rho, \theta)$  in  $S$ . The principle idea can be generalized to other geometric templates, such as circles, and can even be generalized to arbitrary shapes [1].

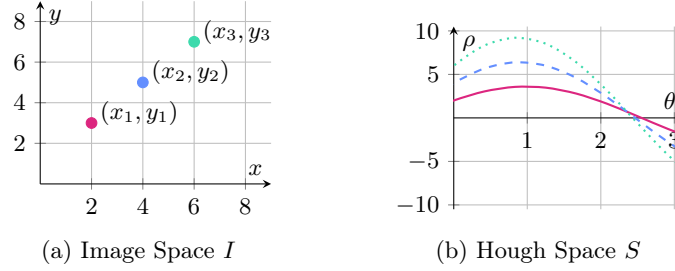


Fig. 1: The Hough transform maps image points (left) to sinusoidal curves in Hough space (right).

Note that the line  $(\rho, \theta + \pi)$  equals the line  $(-\rho, \theta)$ . We can denote this by the equivalence relation  $(\rho, \theta + \pi) \equiv (-\rho, \theta)$  in the Hough space  $S$ . Topologically speaking, we are actually interested in the quotient space  $S/\equiv$ .

In practice this means we limit  $S$  as the  $\rho$ - $\theta$ -plane to  $\mathbb{R} \times [-\frac{\pi}{2}, \frac{\pi}{2})$  and obtain the topology of the Möbius strip.

The standard implementation of the line detection [5] follows a two-step process. First,  $S$  is discretized into an *accumulator array* of size  $n_\rho \times n_\theta$ , where  $n_\rho, n_\theta \in \mathbb{R}$  are application-dependent parameters. Each cell in the accumulator array stores the number of functions passing through it, effectively capturing the vote count for the corresponding line parameters. Second, the accumulator array is exhaustively searched for maximum values, where the corresponding positions indicate parameters of the detected lines.

The Hough transform is widely applied in a various domains, including facial feature detection, object recognition and tracking, and underwater pipeline detection [8]. Its practical utility is reinforced by its implementation in *OpenCV* [2], making it accessible for a range of applications. This implementation differs from the standard original approach, as it does not search for the maximum value in the *accumulator array* to identify for a single specific line. Instead, it applies a threshold relative to the highest *peak*, detecting all lines who exceed this pre-

defined level. This approach makes the method more flexible, allowing multiple lines to be detected.

The performance of the Hough transform is limited by several factors, with its high sensitivity to noise being a major concern. For instance, if a few sampled point deviates from the exact position on the line, the intersection in  $S$  will spread, causing a reduction in *votes* and the appearance of a further peak. As the number of noisy samples increases, multiple intersections accumulate, eventually leading to false positive detections.

## 2.2 Persistent Homology

Topology is a branch of mathematics that studies properties of *objects* that remain unchanged under continuous deformations. At the intersection of data science, computer science and algebraic topology,

TDA is an emerging field that analyzes the topological and geometrical structures of datasets, capturing features such as connected components, loops, and voids.

PH [6,9] is a fundamental tool in Topological Data Analysis (TDA) that can be applied to a wide range of topological structures, including point clouds [6] and images [9]. The key idea behind PH is to describe the evolution of a dataset’s topological features as a parameter continuously varies.

This approach eliminates the need to select a fixed parameter while providing deeper insights by introducing an additional dimension to the analysis.

The combinatorial structures that capture a dataset’s topological features are so-called *complexes*. To construct an evolving sequence of complexes from a topological structure  $X$ , a varying parameter  $r$  must be chosen<sup>3</sup>. For each  $r \leq s$ , we obtain a nested sequence of subcomplexes  $X_0 \subset \dots \subset X_r \subset X_s = X$ , where  $X_r$  is formed by applying the parameter  $r$  on  $X$ .

The resulting sequence of nested subcomplexes is called *filtration*.

**Definition 1 (Sublevelset Filtration).** *Let  $f : X \rightarrow \mathbb{R}$  be a continuous function on a topological space  $X$ . The superlevel-set filtration is the nested sequence of subspaces  $X_r = \{x \in X \mid f(x) \geq r\}$ ,  $\forall r \in \mathbb{R}$ . This filtration satisfies  $X_s \subseteq X_r$ ,  $\forall s \leq r$ , and captures the evolution of topological features as  $r$  varies.*

For image analysis, we represent the input scalar fields as *cubical complexes*, which are topological spaces constructed by joining unit cubes along their faces in a structured way. On these cubical complexes we apply the *superlevel-set* filtration (Definition 1). Intuitively, the process of this particular filtration can be visualized as gradually draining water from a flooded image. As the water level decreases, distinct regions (“islands”) will emerge and progressively merge until the entire underlying structure is revealed.

The resulting sequence of nested subcomplexes structure is transformed into a Persistence Diagram (PD), encoding the evolution of the data’s homological

---

<sup>3</sup> The application of multiparameter persistence is not in the scope of this work.

features derived from the filtration. In the PD (Figure 2 as an example), the topological features are represented based on their *birth* (the parameter value at which they first appear) on the x-axis and their *death* (the moment they merge with more prominent feature) on the y-axis.<sup>4</sup> All points lie above the diagonal, as no feature can die before it is born. A features *persistence*, defined as the difference between its death and birth value, corresponds to its orthogonal distance from the diagonal.

*Remark 1.* The PD can be visualized in various ways. For comparability with other types of filtration, we decided to plot the death over the birth level with decreasing values on both axes.

Features with higher persistence are more significant, whereas those closer to the diagonal are regarded as insignificant, e.g. due to noise. An intuitive analogy can be drawn from alpinism: persistent features resemble prominent mountain peaks. The persistence of a peak is not solely determined by its absolute height but rather how much it stands out relative to its surroundings. An isolated peak remains highly prominent, whereas a tall peak situated near an even taller one appears less significant. Similarly, in persistent homology, features that persist over a long range of the filtration parameter are considered more meaningful than those that quickly vanish.

### 3 Related Work

Several adaptations of the Hough transform have been introduced to mitigate noise-induced uncertainty within the Hough space  $S$ . The Probabilistic Hough transform [12], based on a maximum likelihood assumption, models  $S$  as a probabilistic space. While this approach enhance robustness, it increased computational complexity.

Similarly, the kernel-based Hough transform [7] applies an elliptical-Gaussian kernel to model uncertainty around detected clusters but also introduces additional parameters, requiring fine-tuning.

Another approach to analyzing the Hough space statistically involves the concept of *butterfly shapes* [4,15]. Instead of relying solely on peak detection within the accumulator array, these methods consider the entire surface formed by the intersecting sinusoidal functions, enabling for statistical analysis of peak parameters through interpolation and variance analysis.

From an information-theoretic perspective, voting can be interpreted as a random variable, with values modeled as probability distributions [14,16]. Entropy measures derived from these distributions are further used to estimate peak parameters, potentially enabling a more adaptive detection mechanism.

Additionally, machine learning-based approaches have been explored for line detection, using methods such as Adaptive DBSCAN [10] and trainable Neu-

---

<sup>4</sup> The axis labels for both axes are reversed to ensure compatibility with the visualization of other filtrations.

ral Networks [13], which enhance accuracy and robustness but typically require computational resources, and in some cases, substantial training data.

The discussed approaches all attempt to address the limitations of the original Hough transform, where noise introduces uncertainty in the Hough space, and diffuse accumulations can result in missed detections or false positives. However, each of these methods introduces additional parameters and, more importantly, fails to resolve the fundamental issue: they detect only high peaks rather than truly persistent ones in noisy environments.

## 4 Topology-informed line detection

As outlined in Section 2.1, the voting process for line detection in Hough space  $S$  is highly susceptible to noise in the sampled input image. To address this, we introduce a topology-informed method for line detection in parameter space  $S$ , leveraging PH. This method eliminates the need for additional parameters, while delivering more stable and reliable results.

The PH-based method extends the original Hough transform by building upon the point in the processing procedure where the accumulator array has already been created.

Special attention must be given to the periodicity in Hough space and the defined observation limits. Specifically, the neighborhood of  $\theta = -\frac{\pi}{2}$  at the beginning and  $\theta = \frac{\pi}{2}$  at the end of the period in  $S$  should be considered glued together like a Möbius strip, as already discussed.

That is, the two edges of  $S$ , where  $\theta = -\frac{\pi}{2}$  and  $\theta = \frac{\pi}{2}$  are connected in a diagonally opposing manner (to flip the sign of  $\rho$ ).

The accumulator array derived from  $S$  can be treated as an image, with the voting counts representing the pixel values. Applying the neighborhood definition outlined above, the *superlevel-set* filtration, as described in Section 2.2, is then performed on this array. The resulting PD reveals the most persistent lines in  $S$ : lines with high persistence, indicating significance, are located further from the PDs diagonal, while lines resulting from noise appear closer to the diagonal.

Given the PD, the most persistent features are selected as detected lines. As commonly done [6], noisy topological features near the diagonal, i.e., those with a persistence lower than a threshold  $\nu$ , are filtered out. The remaining features are then mapped back into  $S$ , where the line parameters  $(\rho, \theta)$  are determined for each of them. Although the persistence threshold  $\nu$  does not alter the sum of the parameters, it simply replaces the previous threshold parameter.

In fact, within the PD we can illustrate both, the original and the PH-based voting mechanism, see Figure 2. The original method simply performs a threshold at a specific *birth* level while we propose to perform a threshold at a specific persistence, leading to a thresholding line parallel to the diagonal.

Additionally, the parameter type has shifted from being threshold-dependent on the input data to an introduced parameter  $\nu$ , which is independent of the input and can be used in a “one-size-fits-all” setting. A further key distinction between the original and the proposed method is that, mathematically, our method

tracks the entire evolution of cubical complexes across the varying parameter, while the original method simply constructs only a single cubical complex.

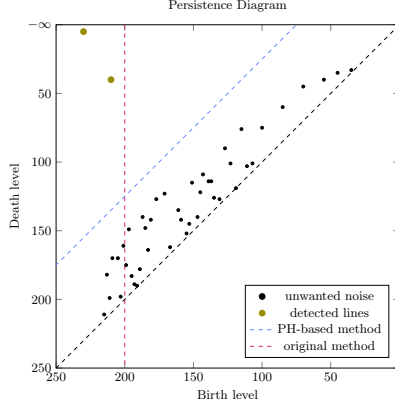


Fig. 2: Schematic comparison of line detection methods: fixed thresholding at a predefined value, as implemented in OpenCV, and adaptive thresholding based on feature persistence derived from PH.

The full advantages of applying PH to the Hough space becomes evident upon examining the PD in Figure 2. In the presence of noise near the *peaks*, the Hough transform’s threshold parameter becomes highly sensitive, leading to false-positive line detections. Adjusting this threshold requires a value-narrow trade-off between detecting all *relevant* lines and avoiding noise-induced artifacts. For example, setting the threshold in this particular example low enough to exclude noise also removes a desired line, while relaxing the threshold to retain both intended lines results in detecting several irrelevant lines. In contrast, the PH-based approach is less sensitive to the chosen parameter  $\nu$ . The persistence of the lines we aim to detect is approximately equal to the number of sampled points per line, while the persistence of noise-induced artifacts corresponds to the expected noise level.

Furthermore, when a line is sampled with fewer points, its corresponding point in the persistence diagram has a lower *birth* value. In a strict thresholding regime, this means that as the number of points decreases, a previously significant feature may fall below the threshold and go undetected. However, due to its diagonal orientation within the PD, the proposed method exhibits greater robustness to a decreasing sampling rate for different lines.

The computation of the PD has a computational complexity of  $O(n\alpha(n))$ , while the filtration is performed in  $O(n \log(n))$ . The storage requirements are linear,  $O(n)$ , where  $n$  denotes the number of complexes.

## 5 Experiments and Evaluation

In the previous Section 4 we showed on the PD, that the original Hough transform has limitations concerning the threshold to be set. From these observations, we derive the following claims: (1) the original Hough transform is more sensitive to increasing noise levels than the PH-based method, causing it to fail at lower noise levels, and (2) at constant noise levels, a decreasing number of points per line compromises the robustness of the original method more than that of the PH-based approach, leading to earlier failure of the original method. Additionally, leveraging PHs mathematical properties, including stability, we further assume that (3) the proposed PH-based method is Lipschitz stable.

We validate our claims with the following experiments<sup>5</sup>, using generated images of the size  $n_w \times n_h = 256 \times 256$  pixels. In the first two experiments, each image contains two parallel *ground truth* lines with slope of  $m = 1$ . The y-intercepts are randomly sampled as  $b \in [50, \dots, 100]$  for the first line, while the second is symmetrically placed at  $-b$ . Each image consists of a set of two-dimensional pixel coordinates  $P = \{(x_i, y_i) \mid 1 \leq i \leq n\}$ , where  $n$  is the experiment dependent number of pixels uniformly sampled along the line. To introduce noise, each point  $P_i$  is perturbed by a normally distributed shift orthogonal to the line,  $p'_i \sim N\left(p_i, \frac{1}{\sqrt{2}}\varepsilon \text{id}\right)$ , where  $\varepsilon$  represents the experiment-dependent noise level and  $\text{id}$  denotes the identity matrix.

As the baseline, we use the *OpenCV* implementation of the Hough transform. For both baseline and our proposed PH-based method, the accumulator array is set to a maximum resolution of 1 pixel for the longest possible  $\rho$  and 1 deg for  $\theta$ , resulting in  $n_\rho = 724$  and  $n_\theta = 180$ .

The parameters – threshold for the original Hough transform and the persistence limit  $\nu$  for the PH-based method – are optimized based on the F1-score, balancing precision and recall.

For all experiments, we report accuracy, precision, and F1-score. A detected line with parameter  $(\rho', \theta')$  is considered correct if it falls within a band around the baseline, define as the target line  $\pm\varepsilon$ . Specifically,  $(\rho', \theta')$  is deemed correct if  $|\rho' - \rho| \leq \varepsilon$  and  $|\theta' - \theta| \leq \frac{2\varepsilon}{n_w}$ .

### 5.1 Robustness against varying noise

In the following experiment, we aim to validate our claim that the proposed PH-based method is more robust to noise than the original method.

To evaluate this, we compare both methods on in detecting two parallel lines under varying noise level  $\varepsilon$ . The lines are both parametrized as described earlier, with  $n_1 = 150$  and  $n_2 = 120$  sampled points, respectively. We generate a dataset of 100 images, each containing randomly sampled noise. The noise levels  $\varepsilon \in [5 \dots 19]$  are uniformly distributed across to ensure a balanced representation of different noise intensities.

<sup>5</sup> The source code for all the experiments is publicly available here: <https://github.com/JRC-ISIA/TopologicalHoughTransformation/>



Table 1: Results of the first two experiments, as described in Sections 5.1 and 5.2.

(a) Comparison of metrics for both variants for 1500 randomly sampled images across varying noise level.

Method	Acc. (%)	Prec. (%)	F1 (%)
PH-based	47.78	91.39	64.66
original	24.67	24.73	39.57

(b) Comparison of metrics for both variants with varying numbers of sampled points in the second line.

Acc. (%)	Prec. (%)	F1 (%)
92.98	95.94	96.36
84.53	87.81	91.62

The results, summarized in Table 1a, show that our method consistently outperforms the original approach across all evaluation metrics.

Figure 3 provides a detailed analysis of the results by noise level. Both the methods exhibit similar performance trends as noise increases. However, the PH-based method demonstrates greater resilience, with its performance degrading more gradually. At a noise level  $\varepsilon = 10$ , the original variant experiences a sharp drop in approaching, whereas the PH-based approach maintains a significant higher performance with only a slight decline.

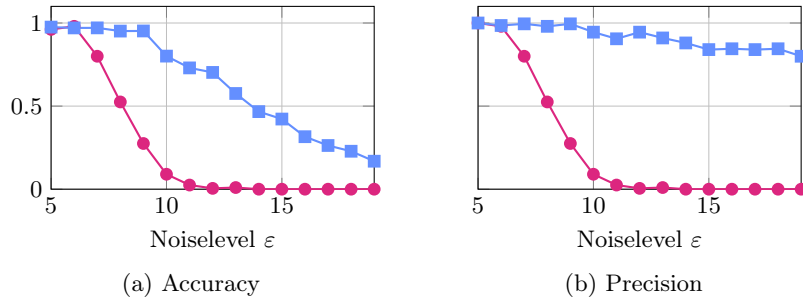


Fig. 3: The results of the experiment targeting our first stated claim, comparing the Accuracy (fig. 3a) and (fig. 3b) of the original- (●) compared with our proposed PH-based method (■). The constant performance of both methods with noise levels  $\varepsilon < 5$  are omitted for brevity.

Figure 4 provides a detailed comparison of both methods on a specific example with a noise level of  $\varepsilon = 8$ . In the image space, our proposed method successfully detects both lines, whereas the original method correctly identifies only one. The underlying reason becomes evident when analyzing the PD: while the PH-based approach detects lines based on the persistence of topological features, the original method effectively *cuts* the PD vertically along the *birth* axis. As discussed in Section 4, this threshold-based approach is highly sensitive to parameter selection and heavily depends on the dataset. The visualization of

the Hough space  $S$  further illustrates the detected lines by highlighting their corresponding intersections along the sinusoidal curves.

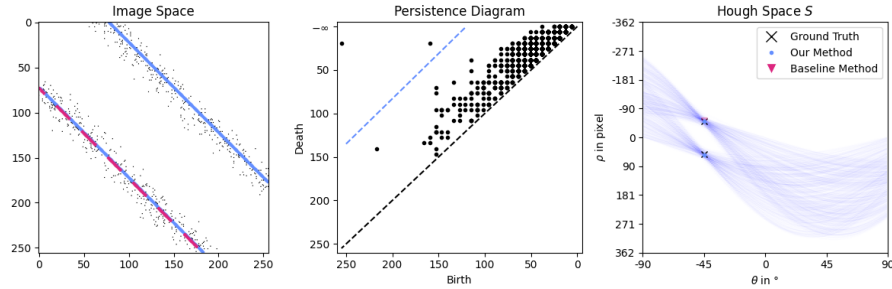


Fig. 4: Result for the experiment with the noised, parallel lines. The first plot shows the sampled points and the one line detected by the original (—) and both lines detected by the PH-based (—) method. The second plot visualizes the PD, highlighting the applied threshold  $\nu$ . The third plot depicts the Hough space  $S$ , illustrating the sinusoidal curves and the corresponding detected lines.

## 5.2 Robustness against irregular number of samples per lines

In this experiment, we validate our second claim that the PH-based method is less sensitive to variations in the number of sampled points per line. To evaluate this, we follow a setup similar to the previous experiment: we use two parallel lines, parametrized as before, with a fixed noise level of  $\varepsilon = 3$ . The first line is always sampled with  $n_1 = 500$  points, while the second line has  $n_2 \in [150 \dots 500]$  in steps of 50. For each value of  $n_2$ , we generate 10 images.

The overall performance across the dataset is summarized in Table 1b. As in the previous experiment, our proposed method consistently outperforms the baseline across all evaluation metrics.

Figure 5 provides a detailed breakdown of performance across varying values of  $n_2$ . It is evident that the original method fails earlier as the number of sampled points in the second line decreases. While the PH-based method also experiences a decline in performance, it maintains a clear advantage over the original variant, exhibiting a much slower degradation.

Figure 6 provides a detailed comparison of both methods for a specific case with  $n_2 = 400$ . In the image space, our method successfully detects both lines, whereas the original variant only detects one. The PD clearly illustrates the reason for the missed detection: the threshold of the original method is set to detect one line, but detecting the second line – given its lower number of sampled points – would require lowering this threshold. However, doing so would also introduce two false positive near the first line. In contrast, the PH-based approach effectively distinguishes true lines from noise.

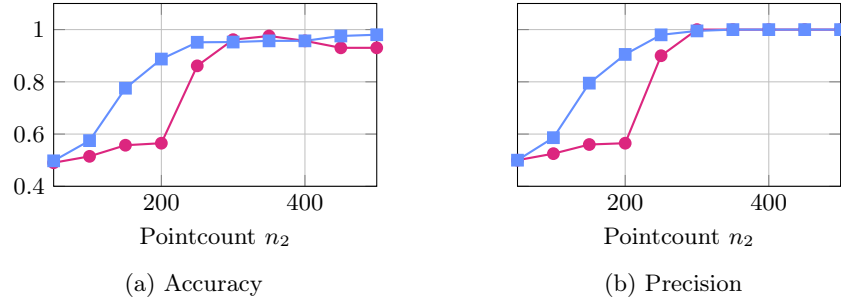


Fig. 5: The results of the experiment targeting our second stated claim, comparing the Accuracy (fig. 5a) and (fig. 5b) of the original- (●) compared with our proposed PH-based method (■).

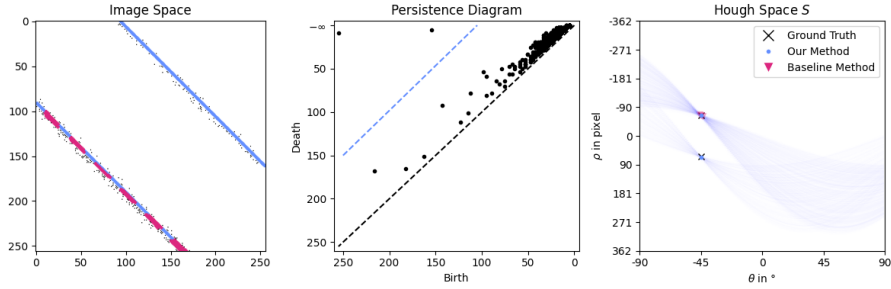


Fig. 6: Result for the experiment with the unevenly sampled, parallel lines. The first plot shows the sampled points and the one line detected by the original (—) and both lines detected by the PH-based (—) method. The second plot visualizes the PD, highlighting the applied threshold  $\nu$ . The third plot depicts the Hough space  $S$ , illustrating the sinusoidal curves and the corresponding detected lines.

### 5.3 Empirical Stability

With our third claim, we argue that the proposed PH-based method exhibits stability properties in the sense of Lipschitz continuity. While we do not attempt to formally prove Lipschitz stability in this work, we provide empirical evidence.

**Definition 2 (Lipschitz Continuity).** *A function  $f : X \rightarrow Y$  mapping from a metric space  $(X, d_X)$  to a metric space  $(Y, d_Y)$  is said to be Lipschitz continuous if there is a constant  $L \geq 0$  such that  $d_Y(f(x_1), f(x_2)) \leq L \cdot d_X(x_1, x_2)$ . for all  $x_1, x_2 \in X$ .*

Lipschitz continuity bounds the effect of input perturbations on the output. A small perturbation in the input leads to a correspondingly small change in the output. It is therefore a notion for stability.

Given our mapping from image space via Hough space to PDs,  $P \xrightarrow{f_1} S \xrightarrow{f_2} PD$ , our aim is to demonstrate that perturbations in the image space, propagated through  $f_1 \circ f_2$  remain bounded by some constant  $L$  within the PDs.

*Remark 2 (Stability of PH).* The mapping of  $f_2$  is already proven to be Lipschitz stable [3]. Therefore, within the chain of mappings, the stability properties of  $f_1$  remain underexplored and are the focus of this experiment.

For this setup, we use a single line parallel to the x-axis with  $n = 50$ , slope  $m = 0$ , y-intercept  $b = 120$ , positioned near the center of the image. In each of 35 iterations, one of the 50 pixel  $p_i = (x_i, y_i)$  is randomly selected (without replacement) and perturbed, generating a new image where  $y'_i \sim N(y_i, 10)$ . This process iteratively transforms the image from a straight line to a noisy version. The experiment is repeated 10 times to evaluate different initial setups. For each iteration, the difference between the original, non-perturbed and the perturbed image is quantified using the 1-Wasserstein distance  $d_W$ , while the *Bottleneck distance*  $d_B$  is applied to the corresponding PDs.

The results are shown in Figure 7, where the bottleneck distance  $d_B$  of the PDs is plotted over the corresponding 1-Wasserstein distance in image space. In Figure 7a, we observe a clear constraint that is never exceeded in the relationship between distance metrics from input to output. The bottleneck distance  $d_B$  converges toward 25 due to the choice of  $n = 50$  and the presence of a high noise regime. Instead of a single significant peak, multiple low-count peaks appear near the diagonal. As a result, the maximal shift distance between two points determines the observed convergence. Figure 7b illustrates the ratio of the bottleneck distance  $d_B$  of the PDs to the Wasserstein distance  $d_W$  of the input. This ratio, derived as a reformulation of Definition 2 in terms of  $L$ , ensures that  $L \geq 1$ , thereby showing Lipschitz continuity in this specific experimental setting. However, when changing the metric on the input images to the bottleneck distance, stability guarantees are no longer provided.

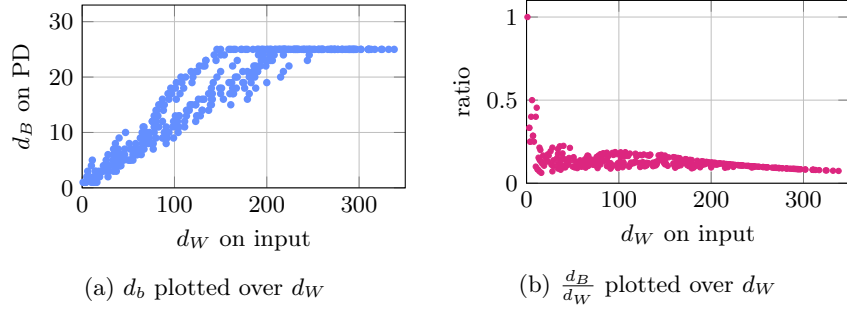


Fig. 7: Scatterplot showing the Bottleneck distance  $d_B$  between the PDs over the 1-Wasserstein distance  $d_W$  of the corresponding point sets in image space. Figure 7a shows  $d_B$  over  $d_W$ , while Figure 7b illustrates the ratio of  $\frac{d_B}{d_W} \leq L$  plotted over  $d_W$ .

## 6 Discussion & Conclusion

The experimental results strongly support the claims in Section 5 on our experimental setups. We demonstrate that increasing noise has less impact on our method compared to the original line detection method. While the original method’s performance rapidly degrades, our approach remains more robust. Additionally, we show that when the number of points on a line decreases while the number of points on another line remains constant, our method remains resilient.

Our third claim addresses the Lipschitz stability of our proposed method. The experiment clearly shows stability when using the 1-Wasserstein distance in the input space. However, the stability argument is not satisfied when using the bottleneck distance between the input images. Achieving stability using the bottleneck distance requires further research.

Despite the compelling results, the proposed PH-based method also has limitations. Computational complexity for line detection increases over to the original Hough transform, as computing the filtration introduces an additional  $O(n \log(n))$  complexity, while constructing the PD adds  $O(n\alpha(n))$ . Moreover, while our experimental results suggest that our method is Lipschitz stable, we lack formal theoretical evidence to support this claim. Yet, this conclusion is limited to the 1-Wasserstein distance metric in the input domain.

Building on this work, we identify a wide range of promising research directions.

A natural extension is to adapt our method for detecting shapes beyond lines, such as curves, circles, and more generally, arbitrary template shapes using the Generalized Hough transform.

Additionally, the integration of the PH-based method with other variants of the original Hough transform, such as the Kernel Hough transform, or the *random sampling* method, presents another compelling avenue for further exploration.

For the proposed PH-based method, we do not provide a formal theoretical proof of its general stability. However, as demonstrated in Section 5.3, our method exhibits empirical stability within the given setting. Nonetheless, we emphasize the importance of conducting a comprehensive stability analysis and developing mechanisms to further enhance its robustness.

In this work, we introduced PH-based method for line detection, a variant of the original Hough transform, that leverages topological structure of the Hough space for more robust line detection. Through our experiments, we demonstrate that the PH-based method outperforms the original Hough transform, exhibiting greater robustness to varying noise levels and different numbers of points per line in the input image. In both experiments, our approach achieved higher detection performance, validating our initial claims.

Beyond its empirical advantages, this work also initiates a discussion on the mathematical stability properties of the Hough transform, a topic that has received little attention. Establishing formal guarantees on stability could further enhance the reliability of the Hough transform in real-world applications.

Moreover, we hope this work will inspire researchers from diverse fields, where PH and TDA are underrepresented, to explore the potential of these tools in their methods. We firmly believe that applying TDA techniques represents a valuable opportunity to generate novel insights across a range of problems. Even those problems considered “solved” may have untapped potential and can benefit from re-examination and further exploration. We hope this work encourages further exploration of TDA in computer vision and beyond.

**Acknowledgments.** The financial support by the Christian Doppler Research Association, the Austrian Federal Ministry for Digital and Economic Affairs and the Federal State of Salzburg is gratefully acknowledged.

## References

1. Ballard, D.: Generalizing the Hough transform to detect arbitrary shapes. *Pattern Recognition* **13**(2), 111–122 (1981)
2. Bradski, G.: The OpenCV Library. *Dr. Dobbs’s Journal of Software Tools* (2000)
3. Cohen-Steiner, D., Edelsbrunner, H., Harer, J.: Stability of Persistence Diagrams. *Discrete & Computational Geometry* **37**(1), 103–120 (Jan 2007)
4. Du, S., Tu, C., van Wyk, B.J., Ochola, E.O., Chen, Z.: Measuring Straight Line Segments Using HT Butterflies. *PLOS ONE* **7**(3), e33790 (2012)
5. Duda, R.O., Hart, P.E.: Use of the Hough transformation to detect lines and curves in pictures. *Communications of the ACM* **15**(1), 11–15 (1972)
6. Edelsbrunner, H., Harer, J.: Persistent homology—a survey. In: *Contemporary Mathematics*, vol. 453, pp. 257–282. American Mathematical Society (2008)
7. Fernandes, L.A., Oliveira, M.M.: Real-time line detection through an improved Hough transform voting scheme. *Pattern Recognition* **41**(1), 299–314 (2008)
8. Hassanein, A.S., Mohammad, S., Sameer, M., Ragab, M.E.: A Survey on Hough Transform, Theory, Techniques and Applications (2015)
9. Huber, S.: Persistent homology in data science. In: *Proc. 3rd Int. Data Science Conference (iDSC’20)*. Data Science – Analytics and Applications, Dornbirn, Austria (virtual) (May 2020)

10. Ke, R., Feng, S., Cui, Z., Wang, Y.: Advanced framework for microscopic and lane-level macroscopic traffic parameters estimation from UAV video. *IET Intelligent Transport Systems* **14**(7), 724–734 (2020)
11. Mukhopadhyay, P., Chaudhuri, B.B.: A survey of Hough Transform. *Pattern Recognition* **48**(3), 993–1010 (Mar 2015)
12. Stephens, R.S.: Probabilistic approach to the Hough transform. *Image and Vision Computing* **9**(1), 66–71 (1991)
13. Vinod, V., Chaudhury, S., Ghose, S., Mukherjee, J.: A connectionist approach for peak detection in Hough space. *Pattern Recognition* **25**(10), 1253–1264 (1992)
14. Xu, Z., Shin, B.S.: Line Segment Detection with Hough Transform Based on Minimum Entropy. In: *Image and Video Technology*. pp. 254–264. Springer (2014)
15. Xu, Z., Shin, B.S.: A Statistical Method for Peak Localization in Hough Space by Analysing Butterflies. In: *Image and Video Technology*. pp. 111–123. Springer (2014)
16. Xu, Z., Shin, B.S., Klette, R.: A statistical method for line segment detection. *Computer Vision and Image Understanding* **138**, 61–73 (2015)